Journal of Vascular Medicine & Surgery
ISSN: 2329-6925

Greene, Vasc Med Surg 2017, 5:3
DOI: 10.4172/2329-6925.1000322

Research Article Open Access

Scaling Laws for Vascular Buckling, Axial and Circumferential: Applications to Pulse Wave Velocity

Peter R Greene*

Bioengineering, BGKT Consulting Ltd, Huntington, NY, 11743, USA

Abstract

Background: Scaling laws for cylindrical column buckling are reviewed, applicable to the cardio-vascular system arteries or veins of various thicknesses to diameter ratios.

Methods: Critical buckling load scales as (hr/L^2) for axial loads, (h/r)^3 for compressive circumferential loads, and (h/r)^0.5 for pulse wave velocity.

Results: Arteries and veins are most susceptible to buckling failure in collapsible tube mode when circumferential hoop stress exceeds external pressure.

Conclusions: Applications include alternating positive (+) and negative (-) wall stresses to investigate the onset of plastic yielding, fatigue, creep, and pulse wave velocity, all relevant to aneurisms, venous thrombosis, hypertension, and arterial sclerosis.

Keywords: Carotid artery tonometry; Column buckling tube wall stress; Stenosis; Aneurism; Varicose veins; Stroke; Collapsible tube dynamics; Hypertension; Stents; Plaque; Thrombosis; Transmural pressure

Introduction

Literature review: In terms of measuring various pulse and cardiac parameters, many different conditions and configurations come into play, including head orientation [1], body posture, stent implants, plaque deposits [2], aneurisms, varicose veins, collapsible tube dynamics [3], stenosis, hypertension, etc. All are relevant to the critical buckling load [4], and elastic response of the arteries. In this report, we attempt to investigate the effects of internal inflation pressure on column buckling load, axial and circumferential.

It is now known that biological tissues respond to the applied stress field, growing preferentially in response to stress (often called "mechanosensing" or "remodeling"). The constant arterial pulse causes the arteries, and to a lesser extent the veins, to be constantly exposed to cyclic loading, where the amplitude of the applied internal pressure is the difference between the systolic and diastolic pressures, typically 40 mmHg to 80 mmHg. Hastings et al. [5] report that thrombosis is directly associated with high shear rates in arteries of various diameters. High shear can be expected in a partially collapsed or buckled vessel.

In terms of pulse wave velocity (PWV) one-dimensional and 3-D models are derived by Van de Vosse et al. [6] showing a travelling pressure wave of the form p(x,t)=po sin(x-ct) where c=wave speed. Weiner et al. [7] derive the 1-D model from the Navier Stokes equations for inviscid flow in tubes. Mirsky [8] and Streeter et al. [9] derive the 1-dimensional pulse wave velocity (PWV) using fundamental mass and momentum conservation principles.

Materials and Methods

Figure 1 shows a hollow tubular column, of radius r, thickness h, length L, and internal pressure p1 (i.e., an inflated vein or artery).

The buckling load in axial compression is given by the Euler buckling equation:

$$F\ crit=\pi^2 \times EI/(L^2) \quad (1)$$

Where F crit=axial buckling force, E=Young's modulus of elasticity, I=column's moment of inertia, L=column length. Boundary conditions for this case are "un-clamped" at each end of the tube. The critical axial buckling load Fcrit is related to the axial wall stress σ_z by the equation $Fcrit=(2\ \pi\ r)\ h \times \sigma_z$. One objective in this report is to estimate the effects of inflating the tube to physiological internal pressure p1, because the inflation pressure will carry part of the axial load.

Results

Including the internal column support tube pressure p1 yields:

$$Fcrit=(\pi\ r^2)\ p1+\pi\ ^2 \times EI/(L^2) \quad (2)$$

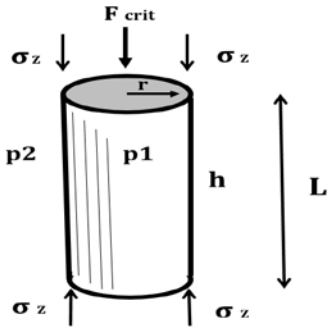

Figure 1: Inflated column of thickness h, length L, and radius r has a critical buckling load of Fcrit=2 **π** r h x $\boldsymbol{\sigma_z}$.

***Corresponding author:** Peter R. Greene, Ph.D., Bioengineering, BGKT Consulting Ltd, Huntington, NY 11743, USA, Tel: +16319355666; E-mail: prgreeneBGKT@gmail.com

Received June 09, 2017; **Accepted** June 26, 2017; **Published** June 29, 2017

Citation: Greene PR (2017) Scaling Laws for Vascular Buckling, Axial and Circumferential: Applications to Pulse Wave Velocity. J Vasc Med Surg 5: 322. doi: 10.4172/2329-6925.1000322

Thus the critical buckling pressure is augmented, so the artery is effectively stronger in axial compression than it would be otherwise. Most in vitro experiments have p1=0.

The moment of inertia I of a tube column is given by:

$$I=\pi \times (r\text{^}3) \times h \quad (3)$$

where I=moment of inertia, r=tube radius, h=tube wall thickness.

Inserting this above yields:

$$Fcrit=(\pi\, r\text{^}2)\, p1+\pi\, \text{^}2 \times E\, [\, \pi \times (r\text{^}3) \times h\,]/(L\text{^}2)$$

Factoring out the cross-sectional area term (π r^2) yields:

$$Fcrit=A\, [p1+\pi^2 E\, (rh/L^2)] \quad (4)$$

Note that Young's modulus E has units of [p.s.i.] the same as pressure p1 [p.s.i.]. The term (Rh/L^2) is a dimensionless parameter characterizing tube geometry. Circumferential Buckling (collapsible tube mode, Figure 2). Han et al. [10] present critical buckling over-pressure for cylindrical tubes as:

$$(p2\text{-}p1)\ crit=\ 0.25\ (h/r)\text{^}3\ [E/(1\text{-}v\text{^}2)] \quad (5)$$

This type of buckling configuration, Figure 2 above, occurs because the circumferential hoop stress is overwhelmed by the external pressure differential (p2-p1). Physiologically, the low-pressure venous system is particularly susceptible to this type of instability.

During buckling, internal tube area, the "lumen", collapses inwards into a two-lobed configuration, Figure 2 above, restricting blood flow. The buckling phenomenon is further accentuated due to Bernoulli effects, because p1 drops to lower values. For Poisson's ratio v=0.5, the circumferential buckling pressure reduces to:

$$\Delta\, p\ crit=\ p2\text{-}p1=0.33\ E\ (h/r)^3 \quad (6)$$

Equation (6) shows that the tendency for a tube to collapse inwards strongly increases with thin-walled and/or larger diameter vessels, such as the vena cava or jugular veins. Note that this external buckling pressure does not depend on tube length L, only the tube thickness to radius ratio (h/r).

Arterial Compliance and Pulse Wave Velocity (PWV). Pulse wave velocity c with units of (meters/sec) is given by (Figure 3).

$$c=sqr[(E/2\ \rho)\ (h/r)] \quad (7)$$

This is the Moens–Korteweg equation, first verified experimentally by Young in 1808-1809. In cases of hardening of the arteries or hypertension, (increasing Young's modulus E for the arteries, with blood density ρ, vessel wall thickness h, and radius r assumed constant),

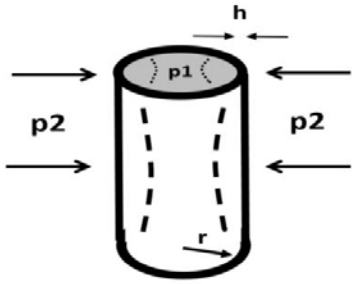

Figure 2: Inward circumferential buckling for tube of radius r, thickness h, caused by excessive transmural pressure (p2-p1)>Pcrit.

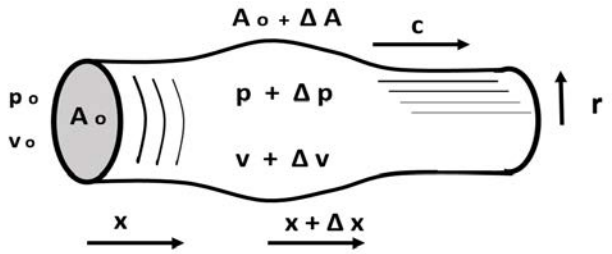

Figure 3: Schematic diagram of pulse velocity **c** in an artery of radius **r**, wall thickness **h.**

it is observed that arterial pulse wave velocity c can increase from 5 m/s to 15 m/s in older individuals.

Experimental data: Shadwick [11] presents data for shark, rat, squid, lobster, toad, snake, tuna, and whale arteries, showing that although the modulus E can vary by a factor of 10X one species to the next, when normalized relative to the average blood pressure, all species have essentially the same elastic moduli for blood vessels, a fundamental result, showing that the vessels remodel the elastic parameters, to meet the demands of the situation. Zhou and Fung [12] measure axial and circumferential elastic moduli for arteries, E_z and E_θ [13].

Greene and Greene [14] present experimental buckling data for tubes of radius 0.25 " (6 mm) , lengths 1" to 6" (2.5 to 15 cm) during axial buckling, yielding Young's moduli in compression of 3 to 14 MPa for Taraxacum and 1600 to 1700 MPa for Hypochaeris plant tubes in vitro. These stem and leaf tubes are inflated in vivo to 1 atmosphere [15-20].

Discussion

Buckling of the arteries or veins, whether axial or circumferential, is important to consider [19,20] because the stress field is locally reversed in sign. Repetitive buckling causes positive (+) and negative (-) alternating wall stress, which can lead to plastic deformation, fatigue, and creep of collagen materials under cyclic load, via the Bauschinger effect.

The extent to which embedded muscle fibers play a role, in terms of maintaining vessel tone and minimizing the fluctuating stress field, remains to be determined.

Collagen material properties are known to vary with temperature, becoming more compliant and susceptible to creep at slightly elevated temperature, just a few degrees above normal body temperature [15] so measurements of this type may prove important.

Lastly, pulse wave velocity c is known to increase in older individuals, an indication of stiffer Young's modulus E for the arteries, and possibly also because of increased wall thickness h caused by plaque deposits. It would be interesting, for instance, to measure the effects of stents on wave velocity. Clinical experiments may include using doppler ultrasound to accurately measure pulse wave velocity.

References

1. Holtackers RJ, Spronck B, Heusinkveld MH, Crombag G, Op t'Roodt J, et al. (2016) Head orientation should be considered in ultrasound studies on carotid artery distensibility. J Hypertens 34: 1551-1555.
2. Teng Z, Feng J, Zhang Y, Sutcliffe MP, Huang Y, et al. (2015) A uni-extension study on the ultimate material strength and extreme extensibility of atherosclerotic tissue in human carotid plaques. J Biomech 5: 3859-3867.
3. Yuan J, Teng Z, Feng J, Zhang Y, Brown AJ, et al. (2015) Influence of material

property variability on the mechanical behaviour of carotid atherosclerotic plaques: A 3D fluid-structure interaction analysis. Int J Numer Method Biomed Eng.

4. Luetkemeyer CM, James RH, Devarakonda ST, Le VP, Liu Q, et al. (2015) Critical buckling pressure in mouse carotid arteries with altered elastic fibers. J Mech Behav Biomed Mater 46: 69-82.
5. Hastings SM, Deshpande SR, Wagoner S, Maher K, Ku DN (2016) Thrombosis in centrifugal pumps: location and composition in clinical and in vitro circuits. The International Journal of Artificial Organs 39: 200-204
6. Van de Vosse FN, Stergiopulos N (2011) Pulse wave propagation in the arterial tree. Annual Review of Fluid Mechanics 43: 467-499.
7. Wiener F, Morkin E, Skalak R, Fishman AP (1966) Wave propagation in the pulmonary circulation. Circulation Research 19: 834-850.
8. Mirsky I (1967) Wave propagation in a viscous fluid contained in an orthotropic elastic tube. Biophysical Journal 7: 165-186.
9. Streeter VL, Keitzer WF, Bohr DF (1963) Pulsatile pressure and flow through distensible vessels. Circulation Research 13: 3-20.
10. Han HC, Chesnutt JK, Garcia JR, Liu Q, Wen Q (2013) Artery buckling: new phenotypes, models, and applications. Annals of Biomedical Engineering.
11. Shadwick RE (1999) Mechanical design in arteries. Journal of Experimental Biology 202: 3305-3313.
12. Zhou J, Fung YC (1997) The degree of nonlinearity and anisotropy of blood vessel elasticity. Proceedings of the National Academy of Sciences 94: 14255-14260.
13. Fung YC, Zweifach BW, Intaglietta M (1966) Elastic environment of the capillary bed. Circulation Research 19: 441-461.
14. Greene PR, Greene VA (2017) Stress, Strain-Rate Analysis of Sub Surface Driveway Plants. Journal Plant Studies 6: 55-64.
15. Frawleya T, Bunton TB (2012), Effect of Temperature on Pulse Wave Velocity and Arterial Compliance J Undergrad Research Physics; pp: 1-10.
16. Goriely A (2017) The Mathematics and Mechanics of Biological Growth. Springer.
17. Grotberg JB, Jensen OE (2004) Biofluid mechanics in flexible tubes. Annual Review of Fluid Mechanics.
18. Hazel AL, Heil M (2003) Steady finite-Reynolds-number flows in three-dimensional collapsible tubes. Journal of Fluid Mechanics 486: 79-103.
19. Morozov NF, Tovstik PE (2010) On modes of buckling for a plate on an elastic foundation. Mechanics of Solids 45: 519-528.
20. Khater ME, Eltaher MA, Abdel-Rahman E, Yavuz M (2014) Surface and thermal load effects on the buckling of curved nanowires. Engineering Science and Technology, an International Journal 17: 279-283.

Appendix I: Arterial Pulse Wave Velocity (PWV).

Speed of sound in air c_0 is typically 350 meters/sec., compared with a much slower pulse wave speed in arteries, in the range 5 to 15 meters/sec, depending on arterial stiffness E. Whether in air or an artery, acoustic mechanics of this type of compressive wave propagation are fundamentally the same (Figure 3).

Pulse wave velocity is derived from a similar acoustic wave equation, given by:

$$\partial^2 p(x,t) / \partial x^2 = -(1/ c^{2)} \partial^2 p(x,t) / \partial t^2 \qquad \text{(A-1)}$$

Solutions to this equation are a matter of a travelling wave of the form:

$$p(x, t)=po \sin (x-ct) \qquad \text{(A-2)}$$

Where wave speed, for an elastic tube, is given by:

$$c=[(E/2\ \rho) \times (h/r)]^{½} \qquad \text{(A-3)}$$

Thus, the stiffer the artery, the faster the wave speed, and the thicker the artery, the faster the wave speed.

As a practical matter, a pressure measuring device is placed at two locations on the body, using an instrumented elastic band secured with Velcro, typically at the upper and lower leg, or the upper and lower arm, in order to measure the wave transit time, which is in the range 0.05 to 0.15 secs for the femoral arteries, and 0.02 to 0.06 secs for the brachial arteries.

At this time, it the effects of a partially buckled artery on pulse wave speed remain uncertain. Experimentally, the buckled configuration can be realized by bending the arm or leg during the pulse velocity (PWV) measurement.